



HAL
open science

A Revised Pseudo-Second-Order Kinetic Model for Adsorption, Sensitive to Changes in Adsorbate and Adsorbent Concentrations

Jay Bullen, Sarawud Saleesongsom, Kerry Gallagher, Dominik Weiss

► **To cite this version:**

Jay Bullen, Sarawud Saleesongsom, Kerry Gallagher, Dominik Weiss. A Revised Pseudo-Second-Order Kinetic Model for Adsorption, Sensitive to Changes in Adsorbate and Adsorbent Concentrations. *Langmuir*, 2021, 37 (10), pp.3189-3201. 10.1021/acs.langmuir.1c00142 . insu-03163152

HAL Id: insu-03163152

<https://insu.hal.science/insu-03163152>

Submitted on 9 Mar 2021

HAL is a multi-disciplinary open access archive for the deposit and dissemination of scientific research documents, whether they are published or not. The documents may come from teaching and research institutions in France or abroad, or from public or private research centers.

L'archive ouverte pluridisciplinaire **HAL**, est destinée au dépôt et à la diffusion de documents scientifiques de niveau recherche, publiés ou non, émanant des établissements d'enseignement et de recherche français ou étrangers, des laboratoires publics ou privés.

A revised pseudo-second order kinetic model for adsorption, sensitive to changes in adsorbate and adsorbent concentrations

^{1*}Jay C. Bullen; ¹Sarawud Saleesongsom; ²Kerry Gallagher; and ^{1,3*}Dominik J. Weiss

¹Department of Earth Science and Engineering, Imperial College London, London SW7 2AZ, United Kingdom

²Géosciences/OSUR, University of Rennes, Rennes, 35042, France

³Civil and Environmental Engineering, Princeton University, United States of America

*Corresponding authors:

Email: j.bullen16@imperial.ac.uk; d.weiss@imperial.ac.uk

Graphical Abstract

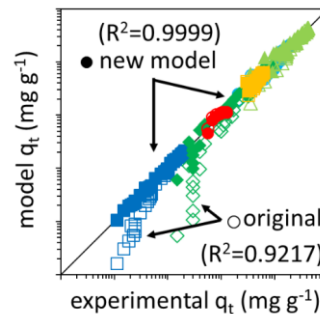
original PSO model

$$\frac{dq_t}{dt} = k_2(q_e - q_t)^2$$



revised PSO model

$$\frac{dq_t}{dt} = k'C_t \left(1 - \frac{q_t}{q_e}\right)^2$$



Keywords

Adsorption kinetics; kinetic model; pseudo-second order; Lagergren; water treatment; particle size

22

Abstract

23 The development of new adsorbent materials for the removal of toxic contaminants from drinking
24 water is crucial to achieving the United Nations Sustainable Development Goal 6 (clean water and
25 sanitation). The characterisation of these materials includes fitting models of adsorption kinetics to
26 experimental data, most commonly the pseudo-second order (PSO) model. The PSO model,
27 however, provides no sensitivity to changes in experimental conditions such as adsorbate and
28 adsorbent concentrations (C_0 and C_s) and consequently is not able to predict changes in performance
29 as a function of operating conditions. Furthermore, the experimental conditionality of the PSO rate
30 constant, k_2 , can lead to erroneous conclusions when comparing literature results. In this study, we
31 analyse 108 kinetic experiments from 47 literature sources to develop a relatively simple
32 modification of the PSO rate equation, yielding:

$$\frac{dq_t}{dt} = k' C_t \left(1 - \frac{q_t}{q_e}\right)^2$$

33 Unlike the original PSO model, this revised rate equation (rPSO) demonstrates the first-order and
34 zero-order dependencies upon C_0 and C_s that we observe empirically. Our new model reduces the
35 residual sum of squares by 66% when using a single rate constant to model multiple adsorption
36 experiments with varying initial conditions. Furthermore, we highlight how the rPSO rate constant k'
37 is more appropriate for literature comparison, highlighting faster kinetics in the adsorption of
38 arsenic onto alumina versus iron oxides. This revised rate equation should find applications in
39 engineering studies, especially since unlike the PSO rate constant k_2 , the rPSO rate constant k' does
40 not show a counter-intuitive inverse relationship with the increasing reaction rate when C_0 is
41 increased.

42 Introduction

43

44 There is a wealth of recent literature concerning the development of novel adsorbent materials for
45 the remediation of contaminated water, such as composite materials offering superior stability ¹,
46 ease of separation from the effluent ^{2 3}, or multifunctional capabilities such as photocatalytic activity
47 ^{4 5}. Energy input typically forms about one third of water treatment plant operation costs ⁶, and if
48 energy efficiencies are to be improved then accurate models of adsorption kinetics (including rate
49 constants) are needed to (a) identify the minimum duration needed for batch treatments and (b)
50 estimate maximum flow rates for column or continuous-flow treatments ⁷. Laboratory experiments
51 can only partially capture the environments in which new adsorbents will operate, and in practice
52 different concentrations of adsorbent (C_s) will be needed to treat different concentrations of
53 contaminant in the influent (C_0). It is thus important that adsorption models are made sensitive to
54 operating conditions, providing predictive capabilities.

55 The pseudo-second order (PSO) rate equation ⁸, popularised by Ho and McKay (1999) ⁹, is probably
56 the most popular model currently used to describe adsorption kinetics ¹⁰. The PSO rate equation
57 takes the form:

$$\frac{dq_t}{dt} = k_2(q_e - q_t)^2$$

58

Equation 1

59 where t is time (minutes), q_t is the amount of adsorbate adsorbed per mass of adsorbent at time t
60 (mg g^{-1}), k_2 is the pseudo-second order rate constant ($\text{g mg}^{-1} \text{min}^{-1}$), and q_e is the amount of
61 adsorbate adsorbed at equilibrium (mg g^{-1}) ⁹.

62 The decrease in the concentration of aqueous adsorbate with time is given by the equation:

$$C_t = C_0 - C_s q_t$$

63

Equation 2

64 where C_t is the concentration of aqueous adsorbate at time t (mg L^{-1}), C_0 is the initial adsorbate
65 concentration at $t=0$ (mg L^{-1}) and C_s is the concentration of adsorbent (g L^{-1}).

66 The PSO model is popular for several reasons. Firstly, it has a simple mathematical form. Secondly,
67 despite being applied by Ho and McKay as a mechanistic model for the bidentate adsorption of
68 copper onto peat ¹¹, the PSO model is able to fit kinetic data for a wide range of systems with
69 different reaction mechanisms ^{9 12 13} (including where diffusion control is to be expected ¹⁴). Thirdly,
70 Equation 1 can be integrated and rearranged to provide linear equations (of the form $y=mx+c$) from
71 which the model parameters k_2 and q_e can be easily obtained by linear regression ¹⁵.

72 However, the PSO model has several important limitations due to the absence of adsorbate and
73 adsorbent parameters within the rate equation, with k_2 and q_e parameters being valid only under
74 the specific experimental conditions under which the PSO model was fitted. The first limitation is
75 that the model cannot predict how adsorption kinetics will change as a function of C_0 and C_s , limiting
76 its application in engineering or optimisation studies. Furthermore, rate constants from different

77 literature sources with different experimental conditions cannot be meaningfully compared: greater
78 values of k_2 do not necessarily indicate adsorbents possessing superior adsorption kinetics.

79 The aim of the present study was to modify the popular PSO equation, introducing sensitivity
80 towards changes in C_0 and C_s , with the objective of both improving predictive capabilities for
81 engineering studies, and normalising rate constants for easier comparison between literature
82 sources. The PSO model does not necessarily reveal insights into the adsorption mechanisms (i.e.
83 whether intraparticle diffusion or chemisorption is the rate determining step)^{13 16}, and our aim was
84 similarly to develop an empirical model, rather than a mechanistic model. We thus conducted an
85 empirical analysis of the adsorption kinetics reported by the literature to assess the influence of C_0
86 and C_s on adsorption rates, and to modify the PSO rate equation accordingly.

87 We used the method of initial rates to determine the order of reaction with respect to both C_0 and C_s
88 (given the possibility for data at later times to disguise the true reaction order¹⁷, such as when
89 slower surface precipitation processes coincide with monolayer adsorption¹⁸). We first performed
90 quality control experiments, investigating various methods for calculating initial rates when the
91 availability of early kinetic data is limited (as per many adsorption experiments). We then compiled a
92 wide range of literature data sets wherein multiple adsorption kinetic experiments with different
93 values of C_0 and C_s are reported (with each data set being a specific adsorbate-adsorbent system)
94 and determined the order of reaction with respect to each variable. We used mineral and organic
95 adsorbents, and metal, inorganic and organic adsorbates, to achieve a model that is generally
96 applicable to a wide range of systems, as per the original PSO model. We built the observed C_0 and
97 C_s dependence into a revised form of the PSO rate equation (which we refer to as *rPSO*) and verified
98 that the rate constants given by this new model are more stable with respect to changes in
99 experimental conditions than the PSO rate constant k_2 . Finally, we used two application studies to
100 assess the potential of this revised PSO model to overcome current limitations: (1) describing
101 multiple experiments with varying values of C_0 and C_s using a single rate constant, and (2) achieving a
102 more meaningful comparison of the adsorption kinetics reported across the literature.

103 Experimental

104

105 Data sets

106 Literature sources that experimentally investigated the influence of C_0 , C_s or particle size upon
 107 adsorption kinetics were compiled and the experimental data tabulated (referenced in the
 108 Supplementary Information: SI Table S1). Both mineral adsorbents and organic adsorbents (activated
 109 carbon and chitosan) were included, however zeolites and metal-organic frameworks (MOFs) were
 110 not since the sorption mechanism of adsorbate trapping within cages might produce contrary
 111 results. None of the literature sources found gave any mechanistic account or mathematical
 112 explanation for observed differences in adsorption kinetics due to varying values of C_0 , C_s or particle
 113 size. The majority of the compiled literature used the PSO model to describe adsorption kinetics.

114 In total 47 literature sources with approximately 100 kinetic experiments were collected. This
 115 includes: 14 literature sources with early kinetic data (where $0 < \frac{q_t}{q_e} < 0.2$) to investigate the
 116 influence of early data availability on calculations of the initial rate; 8 literature sources (9 data sets)
 117 with a total 37 experiments where C_0 is varied; 6 literature sources (8 data sets) with a total 27
 118 experiments where C_s is varied; and 21 literature sources (25 experiments) for the adsorption of
 119 inorganic arsenic onto iron oxide and alumina adsorbents. A data set is considered to be all kinetic
 120 experiments using the same adsorbate-adsorbent system within a single literature source. The
 121 compiled data sets are available elsewhere ¹⁹.

122

123 Mathematical approaches for the determination of initial rates

124 Three approaches towards the calculation of initial rates were compared: (1) the initial slope, (2)
 125 linearised PSO kinetics, and (3) non-linear PSO kinetics.

126 In the initial slope approach, the initial rate ($\frac{\Delta q_t}{\Delta t}$ at $t=0$) was calculated as the slope between the
 127 origin at (0,0) and the earliest available data point at $t>0$ ²⁰.

128 Initial rates were also calculated using the following linearised form of the integrated PSO rate
 129 equation:

$$\frac{t}{q_t} = \frac{1}{k_2 q_e^2} + \frac{t}{q_e}$$

130

Equation 3

131 Kinetic profiles were plotted as $\frac{t}{q_t}$ as a function of t and the linear regression was obtained using the
 132 LINEST function in Excel (where the residual sum of squares between the data points and the linear
 133 regression is minimised). The equilibrium adsorption parameter q_e was obtained via the relationship
 134 $q_e = \frac{1}{m}$ where m is the slope of the linear regression, and k_2 via $k_2 = \frac{1}{c \cdot q_e^2}$ where c is the y-intercept.
 135 The initial rate of adsorption was then calculated through the simplification of Equation 1:

$$136 \text{ Initial rate} = \frac{dq_{t=0}}{dt} = k_2 q_e^2$$

137

Equation 4

138 Uncertainties in k_2 , q_e and the initial rate were calculated by linear propagation of the standard
139 errors in m and c given by the LINEST function.

140 Finally, initial rates were calculated using non-linear PSO kinetics. Non-linear fitting of the PSO model
141 to experimental data was achieved by using Microsoft Excel's Solver function to optimise k_2 and q_e
142 values, minimising the sum of squared residuals between the model and experiment. Uncertainties
143 in k_2 and q_e were calculated using a Monte-Carlo approach with 200 simulations as described by Hu
144 *et al.*²¹.

145 For all literature sources, parameters were recalculated to the same units for ease of comparison: k_2
146 ($\text{g mg}^{-1} \text{min}^{-1}$); q_e (mg g^{-1}); and the initial rate ($\text{mg g}^{-1} \text{min}^{-1}$).

147 The influence of the availability of early kinetic data on the accuracy and precision of initial rates
148 calculated using these three approaches was evaluated as follows. Fourteen data sets containing
149 early kinetic data were collected (defined as adsorption experiments containing data within the
150 range $0 < \frac{q_t}{q_e} < 0.2$). Initial rates were then re-calculated as data points were consecutively removed
151 from the earliest to the latest. A linear regression between the calculated initial rates and the value
152 of $\frac{q_t}{q_e}$ at the first available kinetic data was determined and extrapolated to $\frac{q_t}{q_e} = 0$ to provide a
153 theoretical 'true' initial rate (representing if kinetic data were to be collected within an
154 infinitesimally small time period). This theoretical 'true' initial rate was used as a reference value to
155 determine variation in the calculated initial rate as a function of the availability of early kinetic data.
156 A systematic error was calculated using the average error across all data sets and a random error
157 was calculated as the standard deviation in the error across all data sets. The significance of the
158 differences observed in the initial rate errors given by the three mathematical approaches was
159 determined using the paired samples t-test.

160 After evaluating the three approaches (see Results and Discussion), non-linear PSO kinetics were
161 used to determine initial rates in all subsequent calculations.

162

163 **Determining the order of reaction**

164 The order of reaction with respect to the independent variables C_0 and C_s was calculated as the slope
165 of $\log(\text{initial rate})$ versus $\log(\text{independent variable})$ ²². The order of reaction was calculated for each
166 data set (kinetic experiments using the same adsorbate-adsorbent system within a single literature
167 source), with each data point used within the linear regression representing a single kinetic
168 experiment at a unique value of C_0 or C_s . This is represented by the equation:

$$\text{order of reaction} = \frac{\Delta \log (\text{initial rate})}{\Delta \log (C_0 \text{ or } C_s)}$$

169

Equation 5

170 For each data set, the order of reaction with respect to the independent variable was calculated
171 using the LINEST function in Microsoft Excel. The error for each data set was specified as the
172 standard error of the slope. An average (mean, \bar{x}) order of reaction representing all data sets was

173 calculated, with errors reported as the standard deviation. The dependencies of k_2 and k' upon C_0
 174 and C_s were determined using the same method, only substituting the initial rate with k_2 or k' .

175

176 **Modelling the revised rate equation**

177 Our final rate equation, developed and derived in the Results and Discussion (Equation 11, referred
 178 to as the rPSO), is:

$$\frac{dq_t}{dt} = k' C_t \left(1 - \frac{q_t}{q_e}\right)^2$$

179

Equation 6

180 where the rate constant k' takes the units $L g^{-1} min^{-1}$. As the rPSO rate equation is not easily
 181 integrated, experiments were simulated using Microsoft Excel. The quantity of adsorbate adsorbed
 182 at the n^{th} data point was calculated using the following formula:

$$q_n = q_{n-1} + \left((t_n - t_{n-1}) \cdot \left(k' C_{t(n-1)} \left(1 - \frac{q_{n-1}}{q_e}\right)^2 \right) \right)$$

183

Equation 7

184 The time interval between data points, $(t_n - t_{n-1})$ or Δt , was reduced until the magnitude of Δt had
 185 no significant effect on the results. The rPSO parameters k' and q_e were obtained by non-linear
 186 fitting, using Microsoft Excel's Solver function to minimise the residual sum of squared residuals
 187 between the model and experiment.

188 For all literature sources, parameters were recalculated to the same units for ease of comparison: k_2
 189 ($g mg^{-1} min^{-1}$); q_e ($mg g^{-1}$); and the initial rate ($mg g^{-1} min^{-1}$).

190

191 KERRR

$$\frac{dq_t}{dt} = k_2 (q_e - q_t)^2$$

192

Equation 8

193 where t is time (minutes), q_t is the amount of adsorbate adsorbed per mass of adsorbent at time t
 194 ($mg g^{-1}$), k_2 is the pseudo-second order rate constant ($g mg^{-1} min^{-1}$), and q_e is the amount of
 195 adsorbate adsorbed at equilibrium ($mg g^{-1}$)⁹.

196 The decrease in the concentration of aqueous adsorbate with time is given by the equation:

$$C_t = C_0 - C_s q_t$$

197

Equation 9

198 where C_t is the concentration of aqueous adsorbate at time t ($mg L^{-1}$), C_0 is the initial adsorbate
 199 concentration at $t=0$ ($mg L^{-1}$) and C_s is the concentration of adsorbent ($g L^{-1}$).

200 KERRR

201

202

Application studies

203 In the first application study (evaluating the potential of the rPSO model for predictive applications),
204 6 data sets were used: 3 where C_0 was varied and 3 where C_s was varied. In the first step, values of
205 the equilibrium adsorption capacity (q_e) to constrain the model were obtained by fitting kinetic
206 experiments individually using the PSO and rPSO models (optimising the rate constant and q_e
207 simultaneously to minimise the sum of squared residuals). After constraining q_e to these values, all
208 experiments within the given data set (i.e. experiments with the same adsorbate-adsorbent system
209 but different C_0 or C_s values) were simultaneously fit with the PSO and rPSO models, using a single
210 rate constant (k_2 or k' , depending upon the model) to describe all experiments.

211 In the second application study (evaluating the potential of the rPSO rate constant k' for more
212 meaningful comparisons across the literature), 18 experiments reporting the adsorption kinetics of
213 inorganic arsenic onto iron oxide minerals were collated. Both As(V) and As(III) experiments were
214 included, since no significant difference between the adsorption kinetics was observed. A further 7
215 experiments reporting the adsorption of inorganic arsenic onto alumina (Al_2O_3) were collected for
216 comparison. The particle radius (r) was taken as reported by each study.

217 Results and Discussion

218

219 Determination of the influence of experimental conditions (C_0 and C_s) on the 220 initial rate of adsorption

221

222 Quality control: The calculation of initial rates and setting criteria for the selection 223 of literature data sets

224 Many adsorption experiments reported by the literature begin their collection of kinetic data at high
225 values of $\frac{q_t}{q_e}$, where a significant proportion of the reaction has already been completed. This may be
226 due to challenges in collecting samples quickly (especially when filtering is required) given that many
227 adsorption reactions reach equilibrium in the minutes timescale. Other possible reasons include a
228 lack of appreciation over the time-scale at which adsorption kinetics are best measured, with many
229 papers fitting kinetic models on timescales when the reaction has already plateaued and reached
230 equilibrium.

231 Whilst we chose to investigate the influence of C_0 and C_s using the method of initial rates, the lack of
232 literature reporting early stage kinetic data (i.e. low values of $\frac{q_t}{q_e}$) is a challenge. A popular approach
233 to calculate initial rates is to determine the slope of a line that is tangent to the experimental data
234 curve and passes through the origin at (0,0) ²⁰. However, the later the first kinetic data is collected,
235 the shallower the slope will be, creating a systematic underestimation of the initial rate. In the most
236 extreme case, an infinite delay before collection of kinetic data will yield a slope of zero and
237 subsequently an initial rate of zero. Application of a kinetic adsorption model allows for the
238 extrapolation of adsorption rates to $t=0$, however the accuracy of the calculated initial rates depends
239 upon how closely the experimental data obeys the applied model.

240 We therefore conducted a preliminary experiment to investigate how a limited availability of early
241 kinetic data would influence the accuracy and precision of initial rates calculated using the initial
242 slope or using the original PSO model (given that the PSO model is known to approximately describe
243 a wide range of adsorbate-adsorbent systems ¹²). These results were used to set quality control
244 criteria for which data sets would be included within the investigation of the influence of C_0 and C_s
245 on adsorption kinetics.

246 The literature search identified fourteen data sets satisfying the criteria that $\frac{q_t}{q_e} < 0.2$, a relatively
247 small number, highlighting how most authors fail to collect early kinetic data (SI Figure S1). Initial
248 rates calculated from the slope between the origin and the earliest available data point show the
249 typical systematic underestimation of initial rates when early kinetic data is missing (Figure 1a, with
250 the solid line representing the average of all data sets). In contrast, when calculated using the PSO
251 model, there is no systematic error in the calculation of initial rates when the first kinetic data is
252 collected in the range $0 < \frac{q_t}{q_e} < 0.7$ (Figure 1b,c). In all three approaches, significant variation
253 between data sets is observed, i.e. an error in the initial rate unique to each data set. This error (with
254 dashed lines representing one standard deviation) is approximately constant in the initial slope
255 approach, being significant even when early kinetic data is available. In contrast, this error is

256 insignificant using early kinetic data and either of the PSO approaches, however this error increases
257 in magnitude as early data is sequentially removed.

258 Additionally, the absolute values of the initial rates calculated using the earliest possible kinetic data
259 were compared (i.e. 14 initial rate calculations), with Student's t-test indicating that both linearised
260 PSO kinetics and non-linear PSO kinetics tend to return an initial rate greater than that calculated
261 using the initial slope (with $p=0.87$ and 0.97 respectively). The increase in initial rates calculated
262 using non-linear PSO kinetics versus linearised PSO kinetics is not significant ($p=0.33$ using the 14
263 initial rate calculations). However, when comparing the calculated initial rates with all possible data
264 cut-offs (i.e. 115 initial rate calculations, Figure 1d) the differences are more significant: non-linear
265 PSO kinetics return greater initial rates than linearised PSO kinetics ($p=1.00$). This is due to the
266 biased weighting of linearised PSO kinetics towards data at later times, with the slope of $\frac{t}{q_e}$ versus t
267 increasing as equilibrium adsorption is approached, returning smaller values of q_e and thus giving a
268 smaller initial rate. The difference between initial rates calculated using linearised and non-linear
269 PSO kinetics was observed despite equilibrium adsorption kinetic data from the original literature
270 being excluded in our calculations.

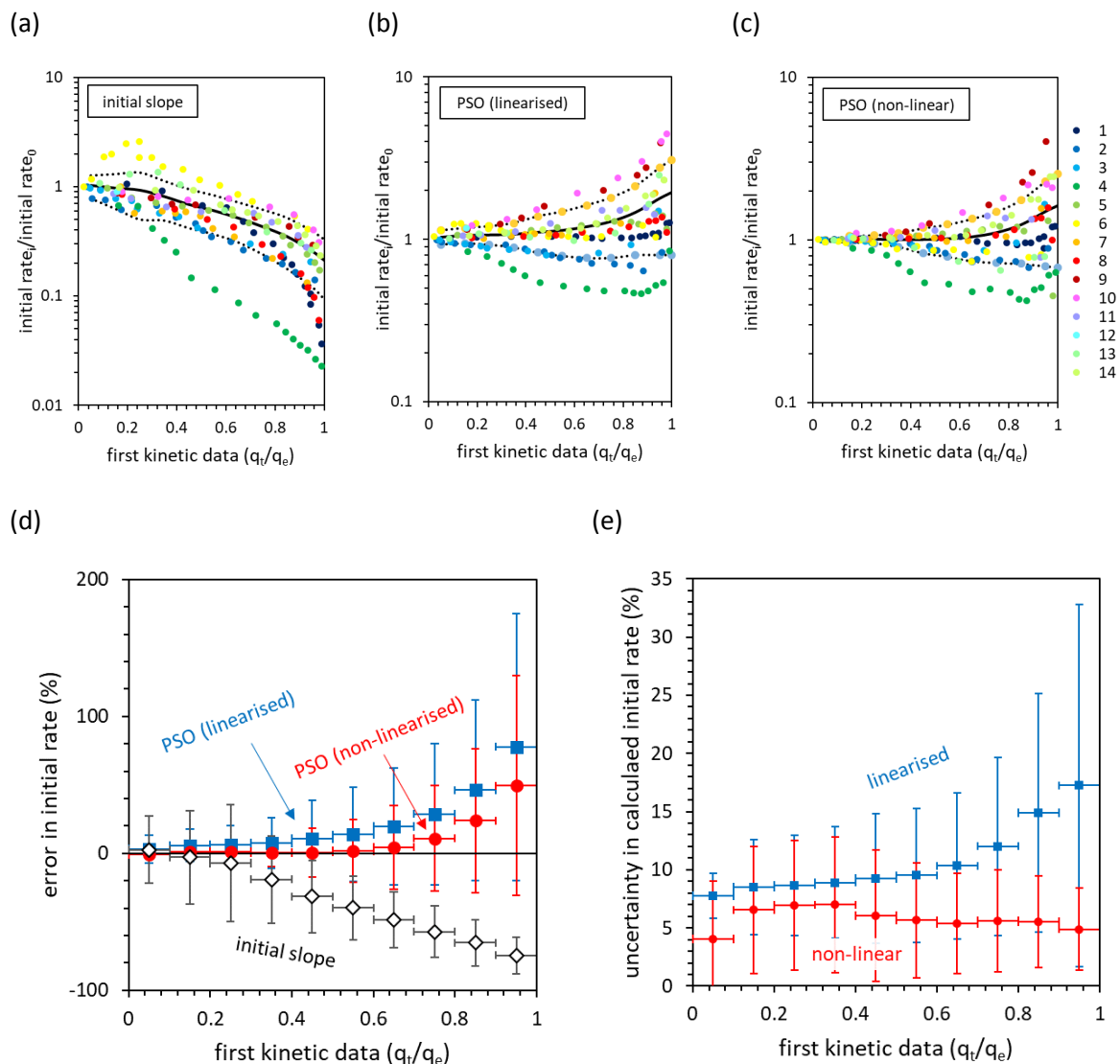
271 Finally, we considered the uncertainties in the initial rates calculated using the two PSO approaches
272 with varying availability of early kinetic data (Figure 1e). The uncertainties in the initial rates
273 calculated using linearised PSO kinetics were calculated from the standard error in the linear
274 regression fit to $\frac{t}{q_t}$ versus t , whilst the uncertainties in non-linear PSO kinetics were calculated using
275 synthetic data and 200 Monte-Carlo simulations²¹. Using linearised PSO kinetics, the propagated
276 uncertainty in the initial rate increases exponentially as early kinetic data is removed. This is
277 explained by how late stage adsorption kinetic data is weighted too heavily when fitting linearised
278 PSO kinetics¹⁰, where the differences in q_t are smaller relative to the measurement uncertainty: this
279 increases the uncertainty of the linear regression. At $\frac{q_t}{q_e} = 0.6$, the average uncertainty in the initial
280 rates calculated using linearised PSO kinetics is 9.5%. In contrast, the uncertainty in the initial rates
281 calculated using non-linear PSO kinetics is essentially independent of the availability of early kinetic
282 data, and at $\frac{q_t}{q_e} = 0.6$ the average uncertainty is only 5.7%.

283 As highlighted here, ideally the data sets used to explore the influence of experimental parameters
284 such as the adsorbate concentration (C_0) and the adsorbent concentration (C_s) should include early
285 kinetic data to reduce the uncertainty in the calculated initial rates. However, literature data
286 reporting early adsorption kinetics is limited. To provide a balance between the accuracy of our
287 initial rate calculations and the collection of a sufficient quantity of data sets for statistical analysis,
288 we set the criterion that data sets must include kinetic data with $\frac{q_t}{q_e} < 0.6$. This boundary condition
289 gives an average error in the calculated initial rate of -44 ± 22 % for the initial slope approach, $+17$
290 ± 38 % using linearised PSO kinetics, and only $+3 \pm 27$ % for the non-linear PSO kinetics. The results
291 indicate that non-linear PSO kinetics are most appropriate for calculating initial rates, with an
292 insignificant systematic error. A ~ 30 % uncertainty remains, associated with how closely the
293 adsorption kinetics fit to the PSO form (with deviations being both due to inaccurate measurements
294 and real chemical mechanisms).

295 By considering a literature source reporting two kinetic experiments only, with a different value of C_0
 296 or C_s in each, a 30% error in the initial rate of the first experiment (as per the boundary condition of
 297 $\frac{q_t}{q_e} < 0.6$) will confer an error of <0.5 in the calculated reaction order. In this work, the average value
 298 of $\frac{q_t}{q_e}$ in the first available kinetic data was 0.37 for experiments where C_0 is varied, and 0.27 for
 299 experiments where C_s is varied. Furthermore, the number of kinetic experiments in each literature
 300 data set was 3-6, indicating that the uncertainties in the calculated initial rates will be $<30\%$. Under
 301 these conditions, the calculated orders of reaction will be accurate to the nearest integer value. This
 302 was deemed appropriate for the purposes of developing the revised PSO model, given that it is
 303 common practice for kinetic adsorption models to use integer values for reaction orders (e.g. the
 304 original PSO equation, and the pseudo-first order kinetic model⁹). In principle, however a similar
 305 analysis could be made relaxing this condition.

306 Consequently, non-linear fitting of the PSO model was used to determine the initial rate of
 307 adsorption in each kinetic experiment in all subsequent work.

308



309 *Figure 1: The influence of the limited availability of early kinetic data on the calculation of initial rates of adsorption,*
310 *assessed by the analysis of 14 literature sources. The influence of removing early kinetic data on the calculated initial rates*
311 *was assessed using (a) the initial slope, (b) linearised PSO kinetics, and (c) non-linear PSO kinetics. The theoretical 'true'*
312 *initial rate is given by initial rate₀ and the initial rate calculated with the available data given by initial rate_c. The solid black*
313 *line represents the average of the 14 data sets, whilst dotted lines indicate one standard deviation. The three approaches*
314 *are compared, assessing the influence of data availability on (d) the relative error in the initial rate, and (e) the uncertainty*
315 *in the calculated initial rate. The horizontal error bars in (d) and (e) represent the size of the bins used for grouping data,*
316 *whilst the vertical error bars indicate the standard deviation calculated between the 14 unique data sets. The data sets*
317 *listed are in order: (1) Yang et al., 2019²³, (2) Yang et al., 2001²⁴, (3 and 4) Liu and Shen, 2008²⁵, (5) Zhu et al. 2016²⁶, (6)*
318 *Yang et al. 2019²⁷, (7) Yang et al. 2019²⁸, (8) Mohamed et al. 2007²⁹, (9) Drenkova-tuhtan et al. 2015³⁰, (10) Liu et al.*
319 *2016³¹, (11) Ornek et al. 2007³², (12) Zhan et al. 2018³³, (13) Ai et al. 2020³⁴, (14) Nadiye-tabbiruka and Sejie 2019³⁵.*

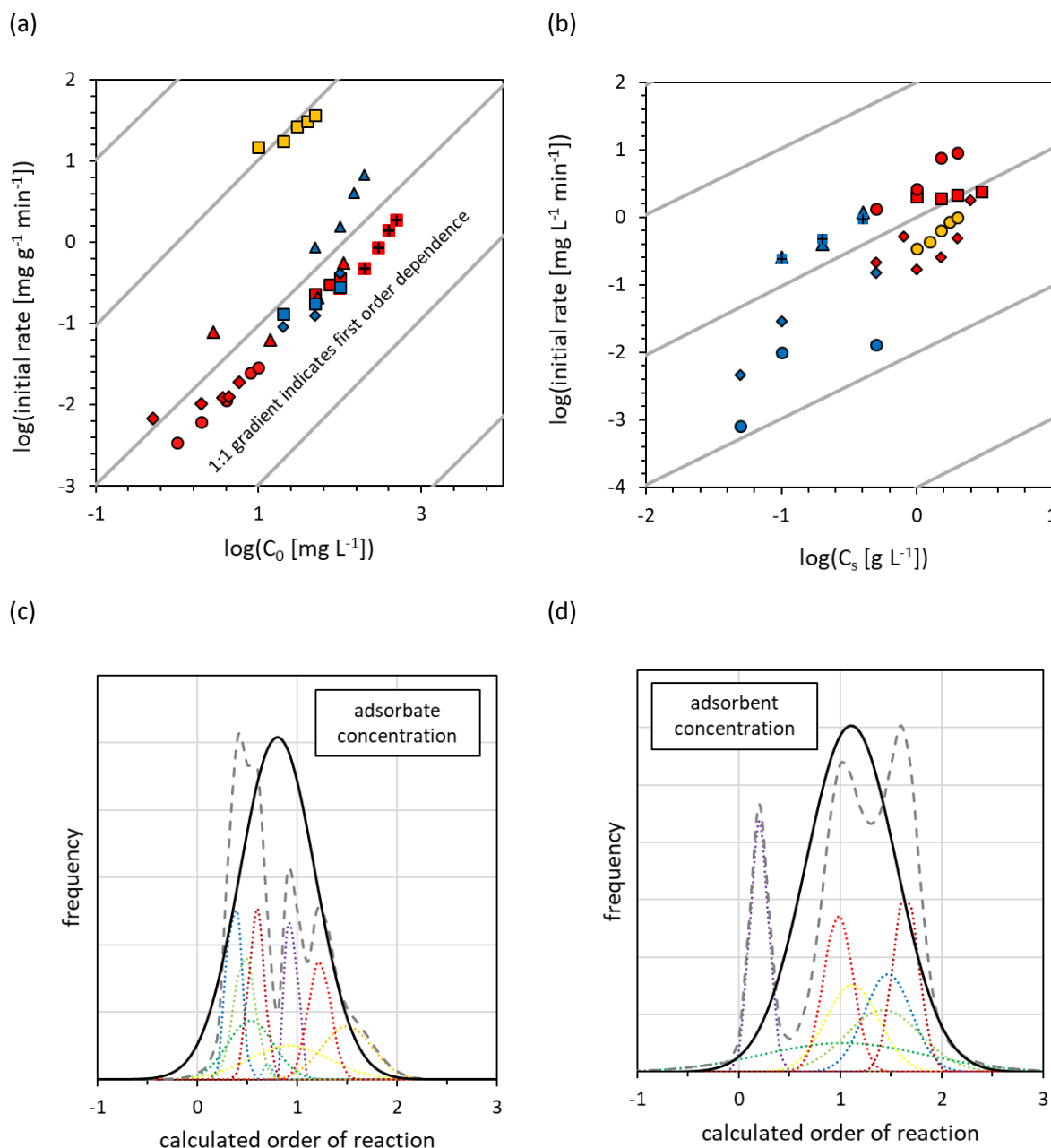
320

321 **Determining the influence of C_0 and C_s upon the rate of adsorption and the PSO** 322 **rate constant k_2**

323 The influence of C_0 and C_s upon the initial rate of adsorption (calculated as the rate at $t=0$ using non-
324 linear PSO kinetics) is presented in Figure 2. For each data set, the order of reaction was determined
325 from the slope of $\log(\text{initial rate})$ versus $\log(C_0)$ or $\log(C_s)$ (Figure 2a,b). Based upon the evaluation of
326 uncertainties in the initial rates calculated using non-linear PSO kinetics (in the previous section), the
327 reaction orders are accurate to the nearest integer value. The data sets tend to show a first-order
328 dependency of initial rate upon the initial adsorbate concentration (C_0) (Figure 2c), with an average
329 dependency and standard deviation of 0.80 ± 0.38 , and a median value of 0.67. Of the 9 data sets, 7
330 were closest to first-order dependency, and 2 were closer to zero-order dependency. The sum of
331 normal distributions representing the reaction orders and uncertainties calculated for each data set
332 was approximated by a single normal distribution. (However, a larger number of data sets are
333 needed to verify this). Based upon the standard deviation and assuming a normal distribution in the
334 results, the relationship between the initial rate and C_0 is first-order with a 90% confidence interval
335 (1.65 standard deviations). This is intuitive for both diffusion and adsorption-controlled mechanisms,
336 as twice as much adsorbate should lead to twice as much adsorbate flux from adsorbent surface into
337 pores, and collisions with the adsorbent surface should be twice as frequent^{36,9}.

338 A first-order dependency of initial rates (normalised to $\text{mg L}^{-1} \text{min}^{-1}$) with respect to the adsorbent
339 concentration (C_s) is also observed (Figure 2d), albeit with a wider distribution of results: an average
340 value of 1.11 ± 0.33 and a median of 1.07. Of the 8 data sets, 6 were closest to first-order
341 dependency, with 1 data set closer to zero-order and another closer to second-order. Based upon
342 the standard deviation and assuming a normal distribution in the results, the relationship between
343 the initial rate and C_s is also first-order with a 90% confidence interval (1.65 standard deviations).
344 This is again intuitive for both diffusion and adsorption-controlled mechanisms, as when C_s is
345 doubled the total surface area available to solution ($\text{m}^2 \text{L}^{-1}$) is doubled, the overall flux of adsorbate
346 entering adsorbent pores is doubled, and the rate of collisions between adsorbate and total
347 adsorbent surface is also doubled. When normalised to mass ($\text{mg g}^{-1} \text{min}^{-1}$) the initial rate is zero-
348 order with respect to C_s , as expected.

349

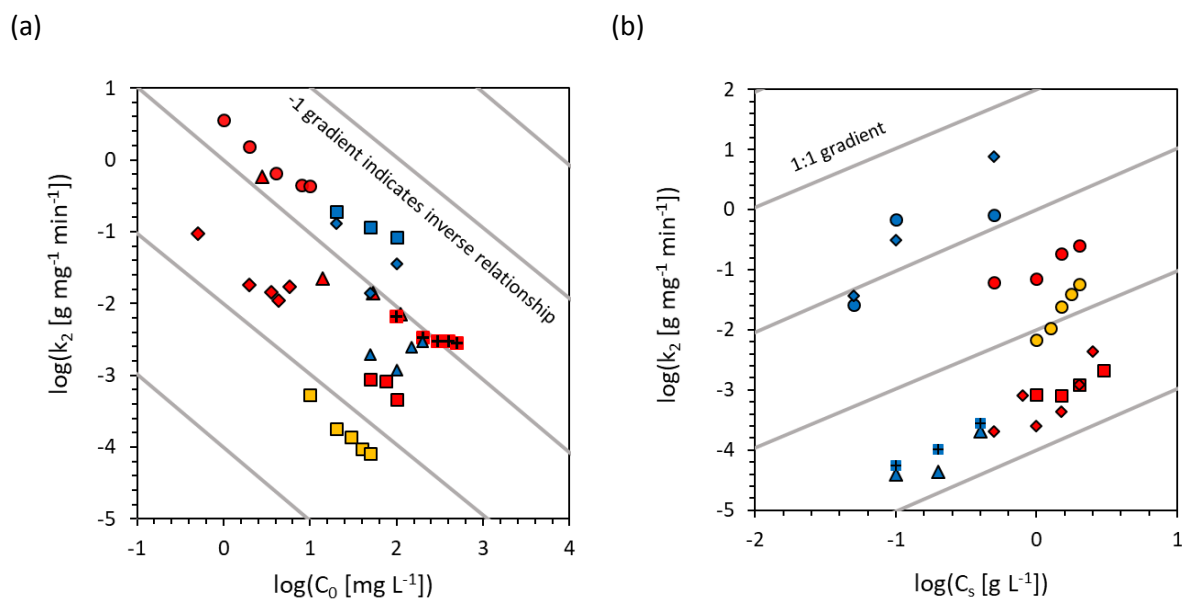


350 *Figure 2: Determining the influence of initial adsorbate concentration (C_0) and adsorbent concentration (C_s) on the initial*
 351 *rate of adsorption using literature data sets. The order of reaction was determined from the slope of $\log(\text{initial rate})$ as a*
 352 *function of (a) $\log(C_0)$ and (b) $\log(C_s)$, with each data point representing a single kinetic experiment (with unique values of C_0*
 353 *and C_s). All experiments in a given data set (one literature paper, where all experimental conditions except for either C_0 or C_s*
 354 *are constant) are grouped by colour and symbol, with oxyanions in red, metal cations in blue, and organic dyes in yellow (a*
 355 *legend referencing the literature sources is presented in SI Figure S2). Uncertainties were calculated from the standard error*
 356 *in the slope. The results are alternatively presented using normal distributions with the mean given by the slope and the*
 357 *standard deviation given by the standard error of the slope (c and d). Here, each data set is represented by a dotted line,*
 358 *and the sum of all data sets given by the dashed line. Solid black lines represent the normal distribution obtained by the*
 359 *average of all data sets.*

360

361 For both predictive modelling and the comparison of adsorption kinetics between literature sources,
 362 it is necessary that rate constants are not affected by the experimental conditions. Whilst adsorption
 363 kinetics are typically first-order with respect to C_0 , the PSO rate constant k_2 is inversely proportional

364 to C_0 (Figure 3a). Consequently, whilst doubling the initial adsorbate concentration typically
 365 increases the initial rate of adsorption by a factor of two, counter-intuitively the PSO rate constant k_2
 366 will decrease by a factor of two. The average slope of $\log(k_2)$ versus $\log(C_0)$ is -0.73 ± 0.46 . The inverse
 367 relationship between k_2 and C_0 is explained by the second-order dependence of the PSO model upon
 368 the **absolute** concentration of available adsorption capacity remaining through the term $(q_e - q_t)^2$. In
 369 cases where the adsorbent is unsaturated, increasing C_0 by a factor of two will approximately double
 370 q_e . The parameter $(q_e - q_t)^2$ at $t=0$ will increase by a factor of four, and consequently k_2 must decrease
 371 by a factor of two to achieve the observed doubling of initial rates.



372 *Figure 3: Dependence of the pseudo-second order (PSO) rate constant k_2 upon (a) initial adsorbate concentration (C_0), and*
 373 *(b) adsorbent concentration (C_s). The data is presented as described in Figure 2, with a legend referencing the literature*
 374 *sources presented in SI Figure S2.*

375

376 In contrast, a positive relationship between C_s and k_2 is observed, with an average dependency of
 377 1.57 ± 0.85 (Figure 3b). (First and second-order dependencies between k_2 and C_s are both included
 378 within the standard deviation). This is explained by how when C_s is doubled, q_e will decrease by a
 379 factor of between 0 and 2: zero when the adsorbate is in excess and q_e is insignificant compared to
 380 C_0 , and two when the adsorbent is in excess and q_e is large relative to C_0 . Consequently, as C_s
 381 increases, $(q_e - q_t)^2$ decreases with a zero-to-second-order dependency, and to achieve the zero-order
 382 relationship between C_0 and initial rates ($\text{mg g}^{-1} \text{min}^{-1}$), k_2 must also increase with a dependency that
 383 is between zero and second-order.

384

385 **Revision of the pseudo-second order (PSO) rate equation to account for**
 386 **changes in adsorbate (C_0) and adsorbent (C_s) concentrations**

387

388 **Modification of the PSO rate equation**

389 In this section, we modify the original PSO rate equation to include the appropriate sensitivity
 390 towards C_0 and C_s , meeting the aims of (a) improving the predictive capacity of this model, and (b)
 391 normalising rate constants for better comparison across the literature.

392 Firstly, for a given concentration of adsorbent, the total concentration of adsorption surface sites is
 393 constant regardless of the value of C_0 . The term within the rate equation used to represent the
 394 contribution of adsorption surface site availability towards the rate of reaction should therefore be
 395 independent of C_0 . The original PSO rate equation contains a second-order dependence upon the
 396 **absolute amount** of adsorption capacity remaining, $(q_e - q_t)^2$, which gives the undesirable inverse
 397 relationship between the rate constant and C_0 demonstrated in Figure 3a. This term can be replaced
 398 with a second-order dependence upon the **relative amount** of adsorption capacity remaining,
 399 $\left(1 - \frac{q_t}{q_e}\right)^2$, which will always return a value of 1 at time $t=0$, independent of C_0 . This term therefore
 400 describes the contribution of adsorption surface site availability towards the rate of adsorption more
 401 appropriately than the original PSO term $(q_e - q_t)^2$. Here, $\frac{q_t}{q_e}$ is the same as the parameter θ used in the
 402 Langmuir adsorption isotherm model²⁰. This modification of Equation 1 gives the following:

403
$$\frac{dq_t}{dt} = k'' \left(1 - \frac{q_t}{q_e}\right)^2$$

404 Equation 10

405 where $k'' = k_2 q_e^2$.

406 The first-order dependence of the reaction rate upon the adsorbate concentration observed
 407 experimentally (Figure 2c) is then defined within the rate equation, giving:

$$\frac{dq_t}{dt} = k' C_t \left(1 - \frac{q_t}{q_e}\right)^2$$

408 Equation 11

409 where $k' = \frac{k_2 q_e^2}{C_0}$. The rate constant k' takes the units $L g^{-1} min^{-1}$.

410 The initial rate of adsorption tends to be zero-order with respect to C_s (when normalised to
 411 adsorbent mass with the units $mg g^{-1} min^{-1}$). The original PSO model gives an initial rate that varies
 412 with changes in C_s , due to its second-order dependence upon the absolute adsorption capacity
 413 remaining $(q_e - q_t)^2$ and the decrease in q_e with increasing C_s . In contrast, since the rPSO depends on
 414 the relative adsorption capacity remaining through the term $\left(1 - \frac{q_t}{q_e}\right)^2$, this rate equation displays
 415 the zero-order dependency of C_s identified from analysis of the literature. The rPSO rate constant k'
 416 is therefore theoretically independent of changes in C_s , unlike the original PSO rate constant k_2 . The

417 rPSO model is similar to the adsorption-only form of the kinetic Langmuir model (kLm), which at high
418 surface coverage is first order with respect to C_t and second order to $(1 - \frac{q_t}{q_e})^{37, 38}$.

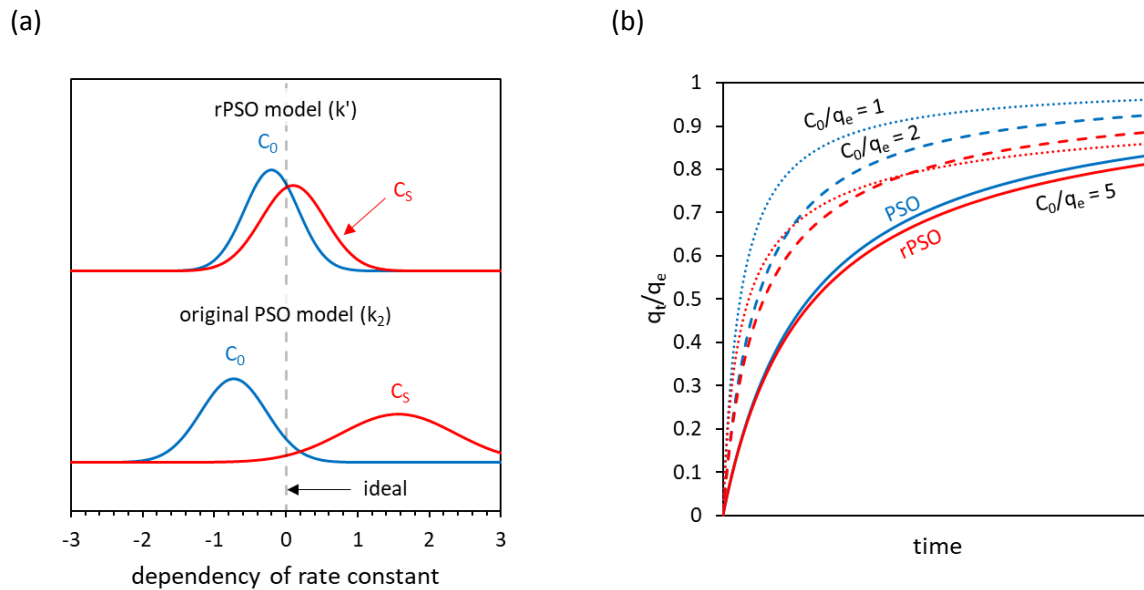
419

420 **Validation of the rPSO rate equation**

421 The removal of experimental conditionality (i.e. the dependency upon C_0 and C_s) from the revised
422 model was verified using experimental data from the literature. The ideal rate constant is unaffected
423 by the experimental conditions, and subsequently the dependency of the rate constant with respect
424 to C_0 and C_s should be zero. These dependencies were calculated from the slope of log(rate
425 constant) versus log(C_0) or log(C_s). As highlighted by Figure 4a, the original PSO rate constant k_2 is
426 strongly dependent upon the experimental conditions, being inversely proportional to C_0 and
427 second-order with respect to C_s . The average C_0 dependency is -0.73 ± 0.46 , and the average C_s
428 dependency is 1.57 ± 0.79 . In contrast, k' is approximately zero-order with respect to both
429 experimental variables. Furthermore, the dependencies of k' upon C_0 and C_s vary less (there is less
430 scattering) than k_2 . The average C_0 dependency is -0.20 ± 0.38 and the average C_s dependency is
431 0.10 ± 0.45 . These results demonstrate that the new rate constant k' is less conditional than k_2 , and
432 that the dependency of adsorption kinetics upon C_0 and C_s is captured by the new model.

433 When the adsorbate is in excess ($q_e < C_0$) the rPSO model approximates the form of the original PSO
434 model. At higher values of q_e relative to C_0 , the graphical form of the two models deviates, due to
435 the rPSO kinetics decreasing more rapidly than PSO kinetics due to the consumption of the
436 adsorption, which decreases the parameter C_t . (However, this effect is logical, given that at low C_t
437 values, the rate of adsorption will be limited by the availability of adsorbate). Therefore, rate
438 constants for the rPSO (k') can be readily calculated from PSO parameters k_2 and q_e when the
439 adsorbate is in excess, using the formula $k' = \frac{k_2 q_e^2}{C_0}$. When the adsorbent removes the majority of
440 the adsorbate, however, the rPSO model will require re-fitting due to the increasing difference in the
441 graphical form of the PSO and rPSO models.

442



443 Figure 4: Verifying that experimental conditionality (with respect to C_0 and C_s) is decreased in the rPSO model versus the
 444 original PSO model. (a) The dependencies of the original PSO rate constant k_2 and the rPSO rate constant k' upon C_0 and C_s
 445 were calculated from the slope of log plots, as per Figure 3, with the ideal rate constant giving a reaction order or
 446 'dependency' of zero. The data is shown as normal distributions with the mean and standard deviation set equal to the
 447 slope and standard error of the slope in the log plots (with 9 data sets for C_0 and 8 for C_s). These values are: -0.73 ± 0.46 for
 448 k_2 and C_0 ; 1.57 ± 0.79 for k_2 and C_s ; -0.20 ± 0.38 for k' and C_0 ; 0.10 ± 0.45 for k' and C_s . (b) A comparison of the form of the
 449 original PSO equation with the rPSO equation, with different $\frac{C_0}{q_e}$ ratios (with $C_s = 1 \text{ g L}^{-1}$). The original PSO model is presented
 450 in blue and the rPSO model in red, with $\frac{C_0}{q_e}$ equal to 1 (dotted lines), 2 (dashed lines), and 5 (solid lines).

451

452

Example applications

453

454

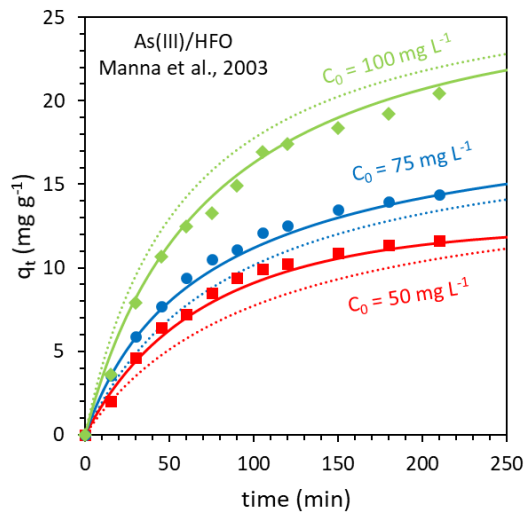
Application 1: Evaluating the predictive capability of the revised PSO model

455 The first objective of this work was to provide a simple modification of the popular PSO model to
 456 introduce predictive capabilities, for the purpose of engineering studies³⁹. If the kinetic model is to
 457 be used to predict adsorption performance under different conditions, then it is essential that the
 458 model parameters obtained experimentally are valid in a range of scenarios. Consequently, we
 459 evaluated whether the rPSO model would provide a better fit to experimental data compared
 460 against the PSO model, if a single rate constant is used to model multiple experiments with different
 461 values of C_0 and C_s .

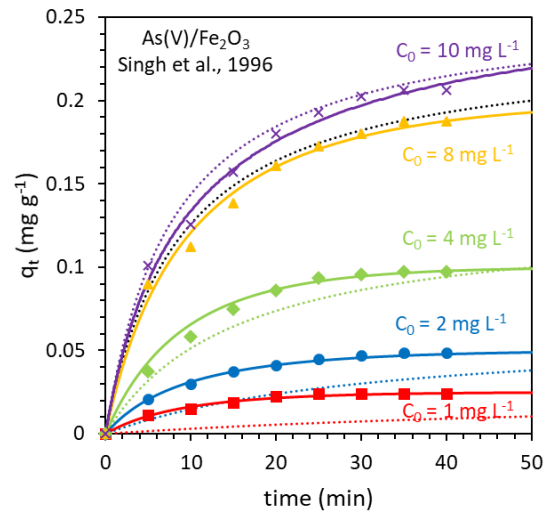
462 The original PSO model tends to systematically overestimate q_t for experiments with high C_0 or low
 463 C_s values and systematically underestimate q_t for experiments with low C_0 or high C_s values (Figure
 464 5). This is due to the negative and positive relationships between k_2 and C_0 and C_s respectively as
 465 previously discussed, with this relationship being denied when a single value of k_2 is used to model
 466 all experiments. The rPSO model gave a better fit to experimental data (i.e. a smaller sum of squared
 467 residuals) in 5 of the 6 data sets tested (all panels in Figure 5 except d) and the median decrease in
 468 the sum of squared residuals when changing from the PSO to the rPSO model was 66%.

469

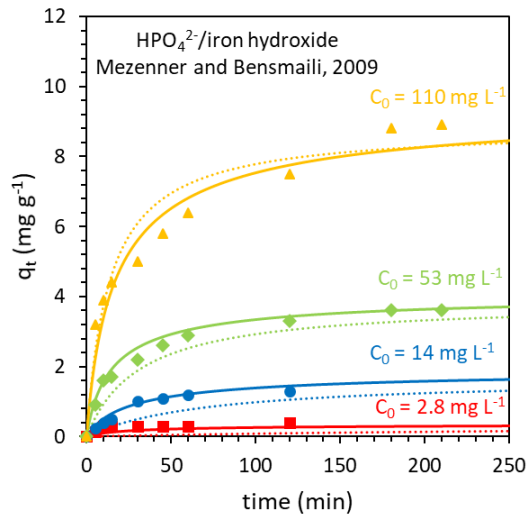
(a)



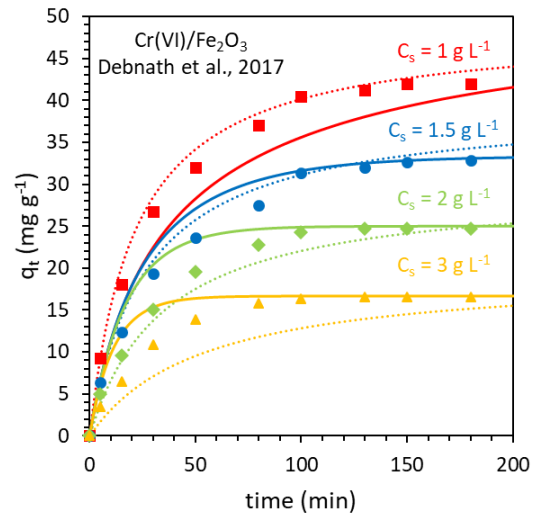
(b)



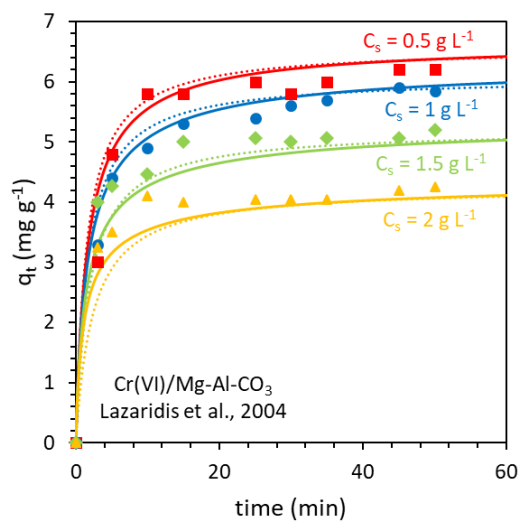
(c)



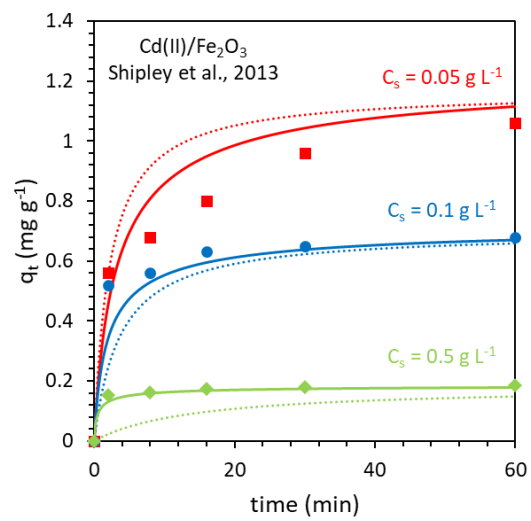
(d)



(e)



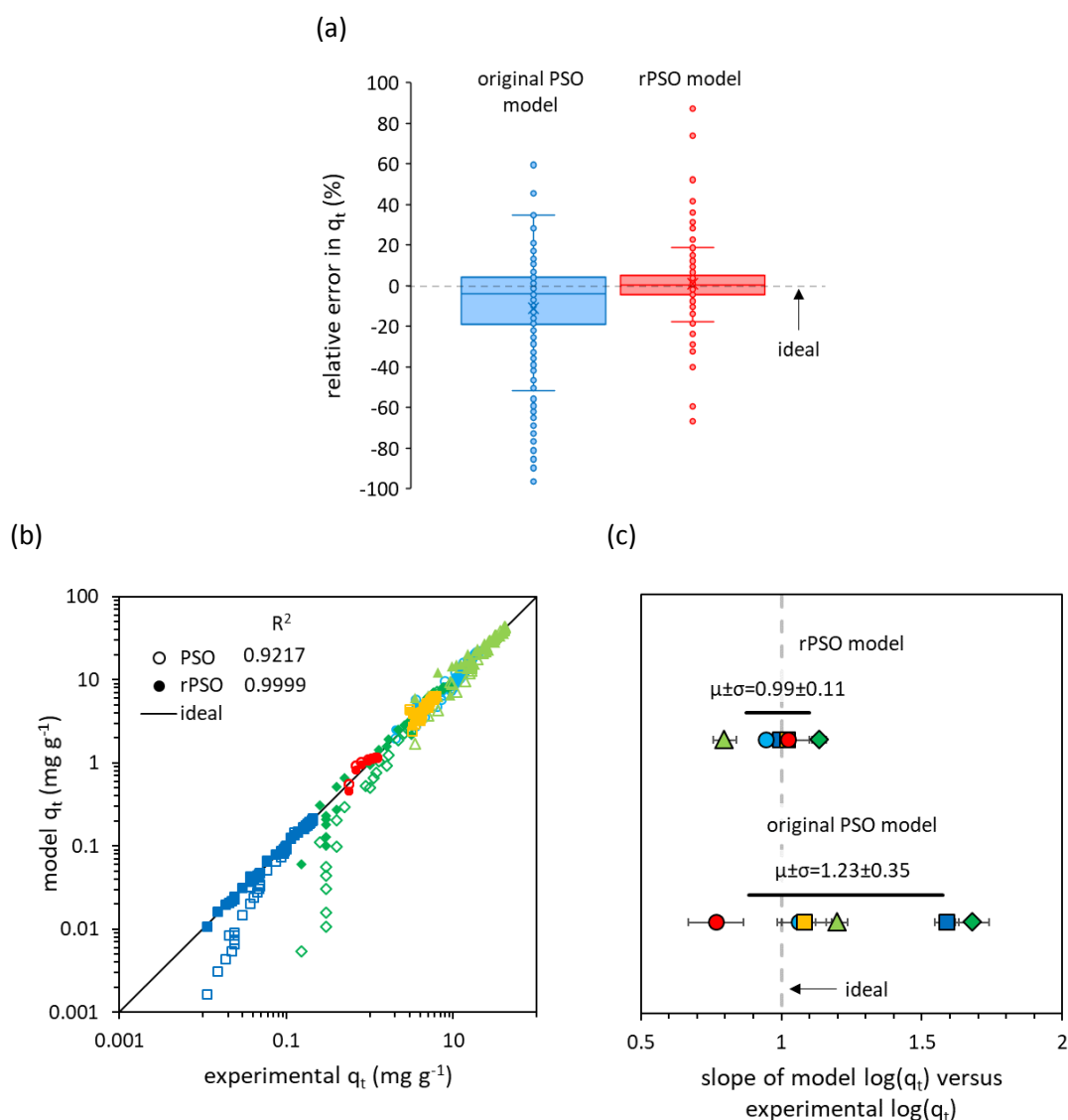
(f)



470 Figure 5: Application study 1: Application of the revised PSO (rPSO) model (solid lines) to describe multiple experiments with
 471 a single rate constant, compared against the original PSO model (dotted lines). (a,b,c) present 3 experiments where C_0 is
 472 varied, and (d,e,f) present 3 experiments where C_s is varied. Experimental data was sourced from Manna et al. (2003)⁴⁰,
 473 Singh et al. (1996)⁴¹, Mezenner and Bensmaili (2009)⁴², Debnath et al. (2017)⁴³, Lazaridis et al. (2004)⁴⁴, and Shipley et al.
 474 (2013)⁴⁵.

475

476 The average relative error of q_t calculated by the rPSO is just $1\pm 17\%$, versus $-11\pm 27\%$ for the original
 477 PSO model (Figure 6a), indicating that the rPSO model provides greater accuracy when modelling
 478 adsorption kinetics with changing values of C_0 and C_s using a single rate constant. Furthermore, the
 479 calibration curve of q_t (model) against q_t (experiment) is closer to the ideal one-to-one line in the
 480 rPSO model, with an R^2 value of 0.999 versus just 0.9217 for the original PSO model (Figure 6b).
 481 Considering each experimental data series in turn, the typical slope of the calibration curve was
 482 closer to one, with less scattering, in the rPSO model (a slope of 0.99 ± 0.11) compared against the
 483 original PSO model (with a slope of 1.23 ± 0.35) (Figure 6c).



484 Figure 6: Application study 1: Cross-calibration of the rPSO model against experimental data (6 literature sources, 22
 485 experiments and 198 data points). (a) Box and whisker plot presenting the relative error of q_t calculated via the original PSO
 486 model and the rPSO model. The boxes highlight the 25%, 50% (median) and 75% percentiles, whilst the whiskers represent

487 the minima and maxima excluding 'outlier' data points, defined as those greater than the top of the box plus 1.5 times the
488 interquartile range, or less than the bottom of the box minus 1.5 times the interquartile range. (b) Cross-calibration plot
489 highlighting the goodness of fit against the one-to-one line. Open shapes indicate q_t values calculated using the original PSO
490 model, whilst filled shapes indicate the rPSO model. Values of R^2 indicate the goodness of fit against the ideal one-to-one
491 line. (c) Comparison of the cross-calibration slopes with each model and each data set. Literature sources are denoted as
492 As(III)/HFO⁴⁰ (dark blue squares), As(V)/Fe₂O₃⁴¹ (light blue circles), HPO₄²⁻/iron hydroxide⁴² (dark green diamonds),
493 Cr(VI)/Fe₂O₃⁴³ (light green triangles), Cr(VI)/Mg-Al-CO₃⁴⁴ (orange squares), and Cd(II)/Fe₂O₃⁴⁵ (red circles). Further results
494 are presented in SI Figure S3.

495

496 Whilst the rPSO rate constant k' appears to be more stable to changes in experimental conditions
497 than the PSO rate constant k_2 , the parameter q_e is conditional, depending upon C_0 and C_s . For
498 predictive modelling, this limitation can be rectified by using an adsorption isotherm to predict q_e
499 (such as the Langmuir or Freundlich model⁴⁶). Though a single value of q_e can be determined for the
500 entirety of each experiment, in scenarios such as a column reactor the equilibrium adsorbate
501 concentration parameter C_e has diminished physical significance, and it may be better to replace this
502 term with C_t , recalculating the hypothetical value of q_e at each point in time. Huang et al. previously
503 demonstrated that this approach can give a better account of the true driving force of the reaction
504 during the initial stages of adsorption⁴⁷.

505

506 **Application 2: Comparison of rate constants between different experimental studies**

507 Comparison of the rPSO rate constant k' is expected to be more meaningful and more appropriate
508 than k_2 when comparing the adsorption kinetics reported in the literature using different
509 experimental conditions, since some of the experimental conditionality (towards changes in C_0 and
510 C_s) is accounted for. To demonstrate the potential application of normalised rate constants towards
511 achieving a meaningful comparison of the adsorption kinetics reported across the literature, we
512 collected 14 and 7 literature sources reporting the kinetics of inorganic arsenic As(V) and As(III)
513 adsorption onto iron oxide and alumina adsorbents respectively.

514 The average value of $\log(k_2)$ for all iron oxide studies is -0.93 ± 1.50 , whilst the average of $\log(k')$ is -
515 1.05 ± 1.08 . In both cases, the standard deviation is large, with more than an order of magnitude
516 variation in k_2 and k' values: neither model provides a rate constant that is generally valid for iron
517 oxide adsorbents used by different studies. Similarly, the adsorption of inorganic arsenic onto
518 alumina gives average values of $\log(k_2) = 0.98 \pm 1.84$ and $\log(k') = 0.35 \pm 1.75$.

519 Whilst the variation in both k_2 and k' across the literature is large, the influence of adsorbent
520 morphology on adsorption kinetics has not been incorporated into either of the PSO and rPSO
521 models. Adsorption kinetics are often faster for adsorbent materials with smaller particles, due to
522 the improved rate of mass transport of the adsorbate to adsorbent surface sites⁴⁸. For instance, in
523 intraparticle diffusion model gives a rate of adsorption that is proportional to r^{-1} (where r is particle
524 size)⁴⁹.

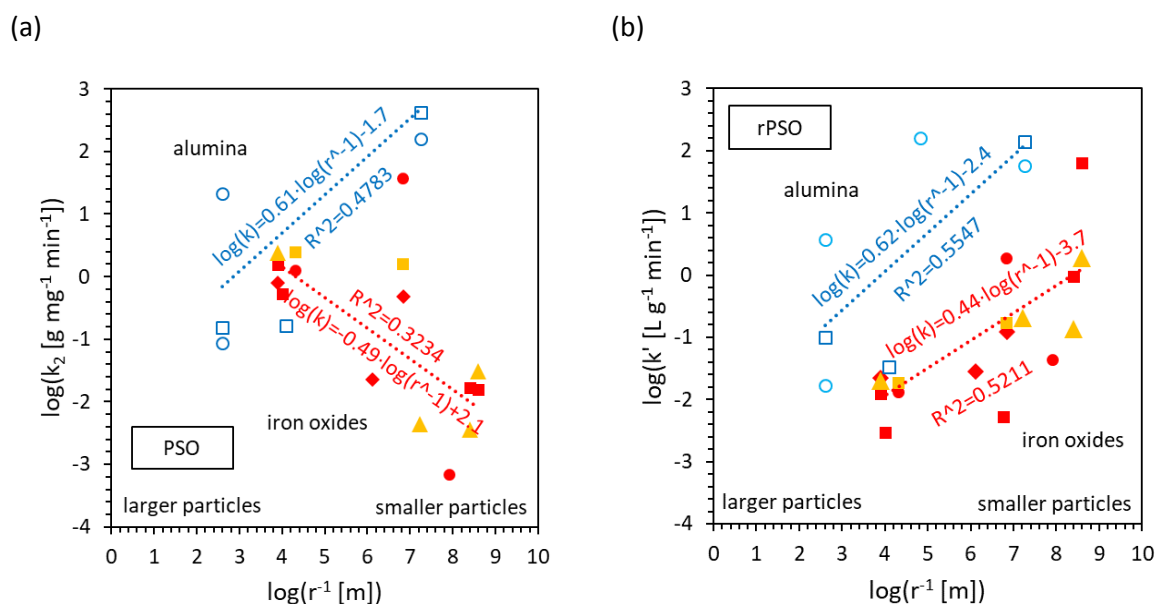
525 Whilst a faster reaction is anticipated for small iron oxide particle sizes, plotting $\log(k_2)$ as a function
526 of $\log(r^{-1})$ shows a weak inverse relationship (linear regression gives a slope of -0.49 ± 0.20 and
527 $R^2 = 0.3234$) (Figure 7a). This is due to the significant increase in q_e as the particle size decreases (SI
528 Figure S4) and the inverse relationship between k_2 and q_e through the term $(q_e - q_t)^2$ as previously

529 discussed. In contrast, alumina shows the anticipated positive relationship (with a slope of 0.61 ± 0.28
 530 and $R^2=0.4783$). Since adsorption onto smaller particles is typically faster than onto larger particles,
 531 the comparison of k_2 values for different adsorbent sizes and different adsorbent materials (i.e. iron
 532 oxides versus alumina) is not useful and is likely to lead to false conclusions.

533 In contrast, we see the anticipated positive relationship for $\log(k')$ as a function of $\log(r^{-1})$ for both
 534 iron oxide and alumina adsorbents (Figure 7b). For the iron oxides we see a slope of 0.44 ± 0.1 with
 535 $R^2=0.5211$, and for alumina we see a slope of 0.62 ± 0.25 and $R^2=0.5547$. The limited goodness of fit in
 536 the linear regression is controlled by factors including poor characterisation of the particle size and
 537 differences in experimental conditions beyond C_0 and C_s , such as the pH. The accurate
 538 characterisation of particle size is especially challenging, given the range of techniques used by the
 539 literature including transmission electron microscopy (TEM), dynamic light scattering (DLS) and sieve
 540 fractionation.

541 The results from this literature survey show greater values of $\log(k')$ at each specific particle size for
 542 alumina versus iron oxides, suggesting that the adsorption of inorganic arsenic is faster onto alumina
 543 than onto iron oxides. With more rigorous analysis, such a study would have important implications
 544 in the design of engineered solutions for arsenic remediation, i.e. opting to use alumina in place of
 545 iron oxides when high flow rates in a column filter are required, or when larger particle sizes are
 546 necessary to achieve the desired flow rate and porosity. This highlights that normalisation of the PSO
 547 rate constant k_2 to the rPSO rate constant k' , or some other constant, can achieve a more
 548 meaningful comparison of the adsorption kinetics reported by the literature.

549



550 *Figure 7: Application study 2: Use of the rPSO rate constant k' to compare literature sources with adsorption kinetics*
 551 *determined under different experimental conditions. Particle size decreases from left to right. Presented are As(V) (red filled*
 552 *shapes) and As(III) (orange filled shapes) adsorption onto iron oxides, and As(V) (dark blue open squares) and As(III) (light*
 553 *blue open circles) adsorption onto alumina. Each data point indicates a different literature source, with a legend given in SI*
 554 *Figure S5.*

Conclusions

555
556
557
558
559
560
561
562
563
564
565
566
567
568
569
570
571
572
573
574
575
576
577
578
579
580
581
582
583
584
585
586
587

This work aimed to modify the popular pseudo-second order (PSO) model of adsorption kinetics to remove experimental conditionality, focusing upon initial adsorbate concentration (C_0) and adsorbent concentration (C_s). A revised PSO rate equation (rPSO) was developed from the empirical analysis of 69 kinetic experiments taken from 15 literature sources. The final equation takes the form $\frac{dq_t}{dt} = k' C_t (1 - \frac{q_t}{q_e})^2$. The first application study demonstrates that the rPSO equation allows for a single rate constant to model multiple experiments, differing in the experimental conditions C_0 and C_s , with greater accuracy and a 66% decrease in the sum of squared residuals versus the original PSO model. The second application study demonstrates that the rPSO equation provides a rate constant which is more useful for comparison across the literature than the PSO rate constant k_2 , obeying the anticipated relationship between adsorption rates and particle size.

The new rate equation is similar to an adsorption-only form of the kinetic Langmuir model (kLm), which at high surface coverage is first order with respect to C_t and second order with respect to $(1 - \frac{q_t}{q_e})$ ^{37 38}. However, the rPSO equation is simpler, with fewer fitting parameters needed, and may thus be more useful for the non-expert. The rPSO equation may prove more useful than the original PSO model in engineering studies where operating conditions are likely to vary.

One of the reasons for the popularity of the original PSO model is its linearised forms, from which k_2 and q_e parameters can be readily obtained from experimental data. Whilst, we have unfortunately not yet found a way to linearise the rPSO rate equation, it is worth noting that linearisation of the original PSO model often results in a poorer quality of fit versus when using non-linear fitting¹⁴. Where necessary, the rate constant for this revised model can be quickly obtained from linearised PSO kinetics using the expression $k' = \frac{k_2 q_e^{\dagger 2}}{C_0^{\dagger}}$.

In our analytical approach, we demonstrate that non-linear fitting of PSO kinetics is more appropriate than linearised PSO kinetics and the initial slope approach when early kinetic data is limited, as is often the case in adsorption experiments. Our literature survey only yielded 9 data sets where C_0 was varied and 8 where C_s was varied, satisfying our requirements for early kinetic data with $\frac{q_t}{q_e} < 0.6$. This highlights a need for experimental work to investigate the influence of these independent variables more systematically, and to ensure that initial adsorption kinetics are adequately captured, given that the method of initial rates is typically considered the superior approach towards determining reaction orders¹⁷.

588 **Acknowledgements**

589 The authors acknowledge support from the Engineering Physical Sciences Research Council (EPSRC)
590 [grant number EP/N509486/1].

591

592 **Supporting information**

593 The supplementary information provides references to all data sets used in this work; figures
594 showing the influence of adsorbent morphology on k_2 ; and tabulates all parameters (q_e , k_2 , k' and
595 initial rate) calculated in this work.

596

597 **References**

- 598 (1) Boddu, V. M.; Abburi, K.; Randolph, A. J.; Smith, E. D. Removal of Copper(II) and Nickel(II) Ions from
599 Aqueous Solutions by a Composite Chitosan Biosorbent. *Sep. Sci. Technol.* **2008**, *43* (6), 1365–1381.
600 <https://doi.org/10.1080/01496390801940762>.
- 601 (2) Linghu, W.; Yang, H.; Sun, Y.; Sheng, G.; Huang, Y. One-Pot Synthesis of LDH/GO Composites as Highly
602 Effective Adsorbents for Decontamination of U(VI). *ACS Sustain. Chem. Eng.* **2017**, *5* (6), 5608–5616.
603 <https://doi.org/10.1021/acssuschemeng.7b01303>.
- 604 (3) Deng, L.; Shi, Z.; Peng, X. Adsorption of Cr(VI) onto a Magnetic CoFe₂O₄/MgAl-LDH Composite and
605 Mechanism Study. *RSC Adv.* **2015**, *5* (61), 49791–49801. <https://doi.org/10.1039/c5ra06178d>.
- 606 (4) D'Arcy, M.; Weiss, D.; Bluck, M.; Vilar, R. Adsorption Kinetics, Capacity and Mechanism of Arsenate and
607 Phosphate on a Bifunctional TiO₂-Fe₂O₃ Bi-Composite. *J. Colloid Interface Sci.* **2011**, *364* (1), 205–212.
608 <https://doi.org/10.1016/j.jcis.2011.08.023>.
- 609 (5) Chi, S.; Ji, C.; Sun, S.; Jiang, H.; Qu, R.; Sun, C. Magnetically Separated Meso-g-C₃N₄/Fe₃O₄: Bifunctional
610 Composites for Removal of Arsenite by Simultaneous Visible-Light Catalysis and Adsorption. *Ind. Eng.*
611 *Chem. Res.* **2016**, *55* (46), 12060–12067. <https://doi.org/10.1021/acs.iecr.6b02178>.
- 612 (6) Smith, K.; Liu, S. Energy for Conventional Water Supply and Wastewater Treatment in Urban China: A
613 Review. *Glob. Challenges* **2017**, *1* (5), 1600016. <https://doi.org/10.1002/gch2.201600016>.
- 614 (7) Dichiara, A. B.; Weinstein, S. J.; Rogers, R. E. On the Choice of Batch or Fixed Bed Adsorption Processes
615 for Wastewater Treatment. *Ind. Eng. Chem. Res.* **2015**, *54* (34), 8579–8586.
616 <https://doi.org/10.1021/acs.iecr.5b02350>.
- 617 (8) Blanchard, G.; Maunaye, M.; Martin, G. Removal of Heavy Metals from Waters by Means of Natural
618 Zeolites. *Water Res.* **1984**, *18* (12), 1501–1507. [https://doi.org/10.1016/0043-1354\(84\)90124-6](https://doi.org/10.1016/0043-1354(84)90124-6).
- 619 (9) Ho, Y. S.; McKay, G. Pseudo-Second Order Model for Sorption Processes. *Process Biochem.* **1999**, *34*
620 (5), 451–465. [https://doi.org/10.1016/S0032-9592\(98\)00112-5](https://doi.org/10.1016/S0032-9592(98)00112-5).
- 621 (10) Simonin, J. P. On the Comparison of Pseudo-First Order and Pseudo-Second Order Rate Laws in the
622 Modeling of Adsorption Kinetics. *Chem. Eng. J.* **2016**, *300*, 254–263.
623 <https://doi.org/10.1016/j.cej.2016.04.079>.
- 624 (11) Ho, Y. S.; McKay, G. The Kinetics of Sorption of Divalent Metal Ions onto Sphagnum Moss Peat. *Water*
625 *Res.* **2000**, *34* (3), 735–742.
- 626 (12) Ho, Y. Review of Second-Order Models for Adsorption Systems. *J. Hazard. Mater.* **2006**, *136* (April
627 2005), 681–689. <https://doi.org/10.1016/j.jhazmat.2005.12.043>.
- 628 (13) Plazinski, W.; Dziuba, J.; Rudzinski, W. Modeling of Sorption Kinetics: The Pseudo-Second Order
629 Equation and the Sorbate Intraparticle Diffusivity. *Adsorption* **2013**, *19* (5), 1055–1064.
630 <https://doi.org/10.1007/s10450-013-9529-0>.
- 631 (14) Xiao, Y.; Azaiez, J.; Hill, J. M. Erroneous Application of Pseudo-Second-Order Adsorption Kinetics
632 Model: Ignored Assumptions and Spurious Correlations. *Ind. Eng. Chem. Res.* **2018**, *57* (7), 2705–2709.
633 <https://doi.org/10.1021/acs.iecr.7b04724>.
- 634 (15) Canzano, S.; Iovino, P.; Leone, V.; Salvestrini, S.; Capasso, S. Use and Misuse of Sorption Kinetic Data: A
635 Common Mistake That Should Be Avoided. *Adsorpt. Sci. Technol.* **2012**, *30* (3), 217–225.
636 <https://doi.org/10.1260/0263-6174.30.3.217>.
- 637 (16) Qiu, H.; Lv, L.; Pan, B. C.; Zhang, Q. J.; Zhang, W. M.; Zhang, Q. X. Critical Review in Adsorption Kinetic
638 Models. *J. Zhejiang Univ. Sci. A* **2009**, *10* (5), 716–724. <https://doi.org/10.1631/jzus.A0820524>.
- 639 (17) Ollis, D. F. Kinetics of Photocatalyzed Reactions: Five Lessons Learned. *Front. Chem.* **2018**, *6* (378), 1–7.
640 <https://doi.org/10.3389/fchem.2018.00378>.

- 641 (18) Lützenkirchen, J.; Behra, P. On the Surface Precipitation Model for Cation Sorption at the (Hydr)Oxide
642 Water Interface. *Aquat. Geochemistry* **1995**, *1* (4), 375–397. <https://doi.org/10.1007/BF00702740>.
- 643 (19) Bullen, J. C.; Saleesongsom, S. Adsorption Kinetics Data Sets, Compiled from the Literature. As Used in
644 the Research Article “A Revised Pseudo-Second Order Kinetic Model for Adsorption, Sensitive to
645 Changes in Adsorbate and Adsorbent Concentrations.” *Zenodo*. January 15, 2021.
646 <https://doi.org/10.5281/ZENODO.4443102>.
- 647 (20) Atkins, P.; Paula, J. De. *Atkins’ Physical Chemistry*, 9th ed.; Oxford University Press, 2009.
648 <https://doi.org/10.1021/ed056pA260.1>.
- 649 (21) Hu, W.; Xie, J.; Chau, H. W.; Si, B. C. Evaluation of Parameter Uncertainties in Nonlinear Regression
650 Using Microsoft Excel Spreadsheet. *Environ. Syst. Res.* **2015**, *4* (1). [https://doi.org/10.1186/s40068-](https://doi.org/10.1186/s40068-015-0031-4)
651 [015-0031-4](https://doi.org/10.1186/s40068-015-0031-4).
- 652 (22) Kirby, M. E.; Bullen, J. C.; Hanif, M. D.; Heiba, H. F.; Liu, F.; Northover, G. H. R.; Resongles, E.; Weiss, D.
653 J. Determining the Effect of PH on Iron Oxidation Kinetics in Aquatic Environments: Exploring a
654 Fundamental Chemical Reaction to Grasp the Significant Ecosystem Implications of Iron Bioavailability.
655 *J. Chem. Educ.* **2019**. <https://doi.org/10.1021/acs.jchemed.8b01036>.
- 656 (23) Yang, H.; Yu, H.; Fang, J.; Sun, J.; Xia, J.; Xie, W.; Wei, S.; Cui, Q.; Sun, C.; Wu, T. Mesoporous Layered
657 Graphene Oxide/Fe₃O₄/C₃N₃S₃ Polymer Hybrids for Rapid Removal of Pb²⁺ and Cd²⁺ from Water.
658 *ACS Omega* **2019**, *4* (22), 19683–19692. <https://doi.org/10.1021/acsomega.9b02347>.
- 659 (24) Yang, X. Y.; Al-Duri, B. Application of Branched Pore Diffusion Model in the Adsorption of Reactive Dyes
660 on Activated Carbon. *Chem. Eng. J.* **2001**, *83* (1), 15–23. [https://doi.org/10.1016/S1385-](https://doi.org/10.1016/S1385-8947(00)00233-3)
661 [8947\(00\)00233-3](https://doi.org/10.1016/S1385-8947(00)00233-3).
- 662 (25) Liu, Y.; Shen, L. From Langmuir Kinetics to First- and Second-Order Rate Equations for Adsorption.
663 *Langmuir* **2008**, *24* (20), 11625–11630. <https://doi.org/10.1021/la801839b>.
- 664 (26) Zhu, Q.; Moggridge, G. D.; D’Agostino, C. Adsorption of Pyridine from Aqueous Solutions by Polymeric
665 Adsorbents MN 200 and MN 500. Part 2: Kinetics and Diffusion Analysis. *Chem. Eng. J.* **2016**, *306*,
666 1223–1233. <https://doi.org/10.1016/j.cej.2016.07.087>.
- 667 (27) Yang, K.; Li, Y.; Zheng, H.; Luan, X.; Li, H.; Wang, Y.; Du, Q.; Sui, K.; Li, H.; Xia, Y. Adsorption of Congo
668 Red with Hydrothermal Treated Shiitake Mushroom. *Mater. Res. Express* **2019**, *7* (1).
669 <https://doi.org/10.1088/2053-1591/ab5ff3>.
- 670 (28) Yang, H.; Wang, Y.; Bender, J.; Xu, S. Removal of Arsenate and Chromate by Lanthanum-Modified
671 Granular Ceramic Material: The Critical Role of Coating Temperature. *Sci. Rep.* **2019**, *9* (1), 1–12.
672 <https://doi.org/10.1038/s41598-019-44165-8>.
- 673 (29) Mohamed, S. F.; Al-Bakri, I. M.; El Sayed, O. H. Biosorption of Lead (II) by Pre-Treated Biomass of
674 Marine Brown Algae *Sargassum Latifolium* and *Sargassum Asperifolium*. *Biosci. Biotechnol. Res. Asia*
675 **2007**, *4* (2), 341–350.
- 676 (30) Drenkova-tuhtan, A.; Mandel, K.; Meyer, C.; Schneider, M. Removal and Recovery of Phosphate from
677 Wastewater with Reusable Magnetically Separable Particles. *IWA Spec. Conf. Nutr. Remov. Recover.*
678 *Mov. Innov. into Pract.* **2015**, No. May. <https://doi.org/10.13140/RG.2.1.1260.8721>.
- 679 (31) Liu, J.; Wu, X.; Hu, Y.; Dai, C.; Peng, Q.; Liang, D. Effects of Cu(II) on the Adsorption Behaviors of Cr(III)
680 and Cr(VI) onto Kaolin. *J. Chem.* **2016**, *2016* (Vi). <https://doi.org/10.1155/2016/3069754>.
- 681 (32) Örneke, A.; Özacar, M.; Şengil, I. A. Adsorption of Lead onto Formaldehyde or Sulphuric Acid Treated
682 Acorn Waste: Equilibrium and Kinetic Studies. *Biochem. Eng. J.* **2007**, *37* (2), 192–200.
683 <https://doi.org/10.1016/j.bej.2007.04.011>.
- 684 (33) Zhan, W.; Xu, C.; Qian, G.; Huang, G.; Tang, X.; Lin, B. Adsorption of Cu(II), Zn(II), and Pb(II) from
685 Aqueous Single and Binary Metal Solutions by Regenerated Cellulose and Sodium Alginate Chemically
686 Modified with Polyethyleneimine. *RSC Adv.* **2018**, *8* (33), 18723–18733.

- 687 <https://doi.org/10.1039/c8ra02055h>.
- 688 (34) Ai, T.; Jiang, X.; Liu, Q.; Lv, L.; Dai, S. Single-Component and Competitive Adsorption of Tetracycline and
689 Zn(II) on an NH₄Cl-Induced Magnetic Ultra-Fine Buckwheat Peel Powder Biochar from Water: Studies
690 on the Kinetics, Isotherms, and Mechanism. *RSC Adv.* **2020**, *10* (35), 20427–20437.
691 <https://doi.org/10.1039/d0ra02346a>.
- 692 (35) Nadiye-tabbiruka, M. S.; Sejie, F. P. Preparation of Coal-Kaolinite Nano Composites and Investigation of
693 Their Use to Remove Methyl Orange from Water. **2019**, *9* (2), 37–43.
694 <https://doi.org/10.5923/j.nn.20190902.01>.
- 695 (36) Largitte, L.; Pasquier, R. A Review of the Kinetics Adsorption Models and Their Application to the
696 Adsorption of Lead by an Activated Carbon. *Chem. Eng. Res. Des.* **2016**, *109*, 495–504.
697 <https://doi.org/10.1016/j.cherd.2016.02.006>.
- 698 (37) Azizian, S. Kinetic Models of Sorption: A Theoretical Analysis. *J. Colloid Interface Sci.* **2004**, *276* (1), 47–
699 52. <https://doi.org/10.1016/j.jcis.2004.03.048>.
- 700 (38) Marczewski, A. W. Analysis of Kinetic Langmuir Model. Part I: Integrated Kinetic Langmuir Equation
701 (IKL): A New Complete Analytical Solution of the Langmuir Rate Equation. *Langmuir* **2010**, *26* (19),
702 15229–15238. <https://doi.org/10.1021/la1010049>.
- 703 (39) Bullen, J. C.; Lapinee, C.; Salaün, P.; Vilar, R.; Weiss, D. J. On the Application of Photocatalyst-Sorbent
704 Composite Materials for Arsenic(III) Remediation: Insights from Kinetic Adsorption Modelling. *J.*
705 *Environ. Chem. Eng.* **2020**, *8* (5). <https://doi.org/10.1016/j.jece.2020.104033>.
- 706 (40) Manna, B. R.; Dey, S.; Debnath, S.; Ghosh, U. C. Removal of Arsenic from Groundwater Using
707 Crystalline Hydrous Ferric Oxide (CHFO). *Water Qual. Res. J. Canada* **2003**, *38* (1), 193–210.
708 <https://doi.org/10.2166/wqrj.2003.013>.
- 709 (41) Singh, D. B.; Prasad, G.; Rupainwar, D. C. Adsorption Technique for the Treatment of As(V)-Rich
710 Effluents. *Colloids Surfaces A Physicochem. Eng. Asp.* **1996**, *111* (1–2), 49–56.
711 [https://doi.org/10.1016/0927-7757\(95\)03468-4](https://doi.org/10.1016/0927-7757(95)03468-4).
- 712 (42) Mezenner, N. Y.; Bensmaili, A. Kinetics and Thermodynamic Study of Phosphate Adsorption on Iron
713 Hydroxide-Eggshell Waste. *Chem. Eng. J.* **2009**, *147* (2–3), 87–96.
714 <https://doi.org/10.1016/j.cej.2008.06.024>.
- 715 (43) Debnath, A.; Bera, A.; Chattopadhyay, K. K.; Saha, B. Facile Additive-Free Synthesis of Hematite
716 Nanoparticles for Enhanced Adsorption of Hexavalent Chromium from Aqueous Media: Kinetic,
717 Isotherm, and Thermodynamic Study. *Inorg. Nano-Metal Chem.* **2017**, *47* (12), 1605–1613.
718 <https://doi.org/10.1080/24701556.2017.1357581>.
- 719 (44) Lazaridis, N. K.; Pandi, T. A.; Matis, K. A. Chromium(VI) Removal from Aqueous Solutions by Mg-Al-CO₃
720 Hydrotalcite: Sorption-Desorption Kinetic and Equilibrium Studies. *Ind. Eng. Chem. Res.* **2004**, *43* (9),
721 2209–2215. <https://doi.org/10.1021/ie030735n>.
- 722 (45) Shipley, H. J.; Engates, K. E.; Grover, V. A. Removal of Pb(II), Cd(II), Cu(II), and Zn(II) by Hematite
723 Nanoparticles: Effect of Sorbent Concentration, PH, Temperature, and Exhaustion. *Environ. Sci. Pollut.*
724 *Res.* **2013**, *20* (3), 1727–1736. <https://doi.org/10.1007/s11356-012-0984-z>.
- 725 (46) Ayawei, N.; Ebelegi, A. N.; Wankasi, D. Modelling and Interpretation of Adsorption Isotherms. *J. Chem.*
726 **2017**, *2017*. <https://doi.org/10.1155/2017/3039817>.
- 727 (47) Huang, Y.; Farooq, M. U.; Lai, S.; Feng, X.; Sampranpiboon, P.; Wang, X.; Huang, W. Model Fitting of
728 Sorption Kinetics Data: Misapplications Overlooked and Their Rectifications. *AIChE J.* **2018**, *64* (5),
729 1793–1805. <https://doi.org/10.1002/aic.16051>.
- 730 (48) Cooney, D. O.; Adesanya, B. A.; Hines, A. L. Effect of Particle Size Distribution on Adsorption Kinetics in
731 Stirred Batch Systems. *Chem. Eng. Sci.* **1983**, *38* (9), 1535–1541. https://doi.org/10.1007/978-1-4419-8074-8_10.
732

733 (49) Simonin, J.; Boute, J. Intraparticle Diffusion-Adsorption Model to Describe Liquid/Solid Adsorption
734 Kinetics. *Rev. Mex. Ing. Quim.* **2016**, *15* (1), 161–173.

735